

Some computational aspects of stochastic phase-field models

Omar Lakkis

Mathematics – University of Sussex – Brighton, England UK

based on joint work with
M.Katsoulakis, G.Kossioris & M.Romito
17 November 2009

3rd
W
O
R
D
S



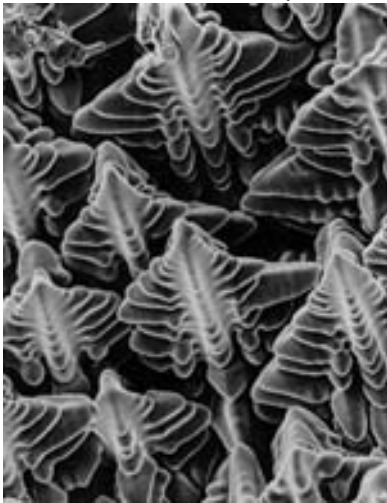
Outline

- 1 Motivation
- 2 Background
- 3 White noise
- 4 Numerical method
- 5 Convergence
- 6 Benchmarking
- 7 Conclusions
- 8 References

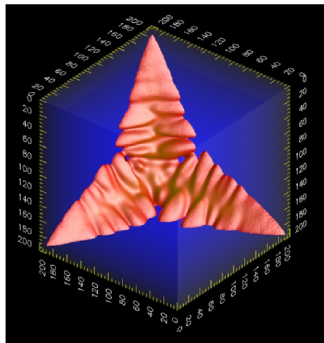
Motivation

Dendrites

A **real-life dendrite** lab picture:

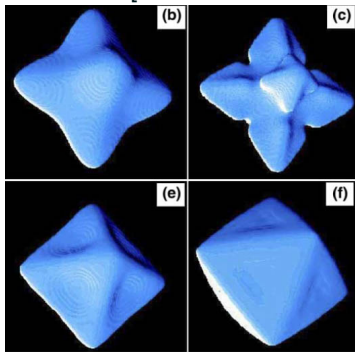


A **phase-field** simulation:

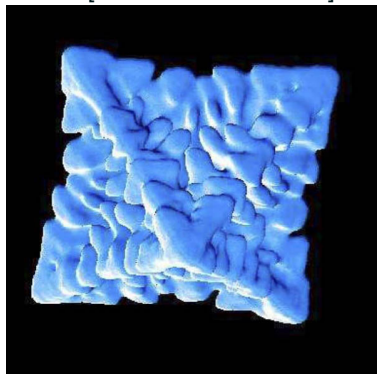


Dendrites

Computed dendrites **without thermal noise** [Nestler et al., 2005]



A computed dendrite **with thermal noise** [Nestler et al., 2005]



Deterministic Phase Field

following [Chen, 1994]

Phase transition in **solidification** process

$$\begin{aligned}\alpha\epsilon\partial_t u - \epsilon\Delta u + (u^3 - u)/\epsilon &= \sigma w && \text{("interface" motion)} \\ c\partial_t w - \Delta w &= -\partial_t u && \text{(diffusion in bulk),}\end{aligned}$$

where

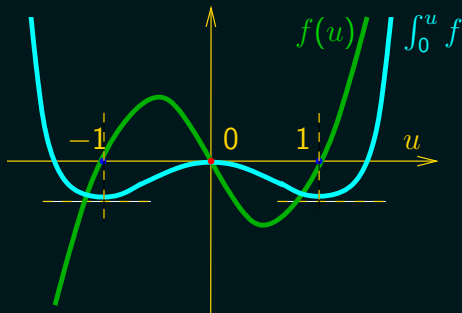
$$u : \text{order parameter/phase field} \begin{cases} \approx 1 & \text{solid phase,} \\ \in (-1 + \delta_\epsilon, 1 - \delta_\epsilon), & \text{interface (region)} \\ \approx -1 & \text{liquid phase.} \end{cases}$$

w : temperature in liquid/solid bulk

The Stochastic (or Noisy) Allen-Cahn Problem

is the following semilinear parabolic stochastic PDE with additive white noise

$$\begin{aligned}\partial_t u(x, t) - \Delta u(x, t) + f_\epsilon(u(x, t)) &= \epsilon^\gamma \partial_{xt} W(x, t), & x \in (0, 1), t \in \mathbb{R}^+ \\ u(x, 0) &= u_0(x), & x \in (0, 1) \\ \partial_x u(0, t) = \partial_x u(1, t) &= 0, & t \in \mathbb{R}^+.\end{aligned}$$



$f_\epsilon(\xi) = \frac{1}{\epsilon^2} (\xi^3 - \xi)$: first derivative of double well potential

$\epsilon \in \mathbb{R}^+$: “diffuse interface” parameter

$\gamma \in \mathbb{R}$: noise intensity parameter

$\partial_{xt} W$: space-time white noise



Why do we care?

about the (deterministic) Allen–Cahn

$$\partial_t u - \Delta u + \frac{1}{\epsilon^2} (u^3 - u) = 0$$

- **Phase-separation** models in metallurgy [Allen and Cahn, 1979].
- **Simplest model** of more complicated class [Cahn and Hilliard, 1958].
- **Cubic nonlinearity approximation** of “harder” (logarithmic) potential.
- **Double obstacle** can replace cubic by other.
- **Phase-field models** of phase separation and **geometric motions** [Rubinstein et al., 1989], [Evans et al., 1992], [Chen, 1994], [de Mottoni and Schatzman, 1995], ...;
- **Metastability**, exponentially slow motion in $d = 1$, [Carr and Pego, 1989], [Fusco and Hale, 1989], [Bronsard and Kohn, 1990];

Why do we care?

about the **stochastic Allen–Cahn**

$$\partial_t u - \Delta u + \frac{1}{\epsilon^2}(u^3 - u) = \epsilon^\gamma \partial_{xt} W$$

- **Noise = stabilizing/destabilizing mechanism** [Brassesco et al., 1995], [Funaki, 1995].
- **Stochastic 1d**: Basic existence theory [Faris and Jona-Lasinio, 1982].
- **Stochastic MCF of interfaces** colored space-time/time-only noises possible [Souganidis and Yip, 2004], [Funaki, 1999], [Dirr et al., 2001].
- **Rigorous mathematical setting** to noise-induced dendrites.

Why do we care?

Modeling and computation with stochastic Allen–Cahn

Stochastic Allen–Cahn (aka Ginzburg–Landau) with noise in materials science:

Modeling in phenomenological/lattice approximation, noise = unknown meso/micro-scopic fluctuation with known statistics effect in macroscopic scale [Halperin and Hoffman, 1977], [Katsoulakis and Szepessy, 2006, cf.];

Simulation noise as ad-hoc nucleation/instability inducing mechanism [Warren and Boettinger, 1995, Nestler et al., 2005, e.g.];

Numerics for $d = 1$ SDE approach [Shardlow, 2000], spectral methods [Liu, 2003], interface nucleation/annihilation [Lythe, 1998, Fatkullin and Vanden-Eijnden, 2004].

Numerics for $d \geq 2$?

Deterministic Allen–Cahn in 1 dimension

metastability and profiles

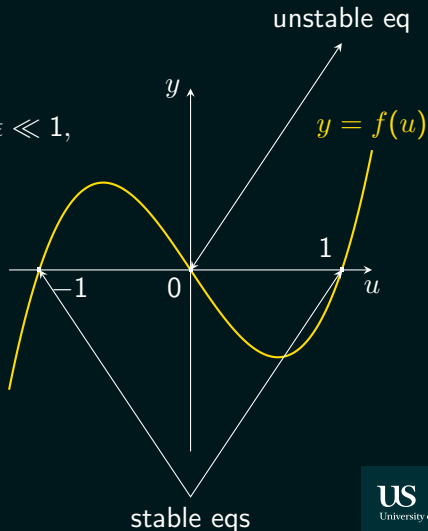
$$\text{PDE: } \partial_t u - \Delta u + \frac{1}{\epsilon^2} f(u) = 0, \quad 0 < \epsilon \ll 1,$$

$$\text{potential: } \frac{1}{\epsilon^2} f(\xi) = \frac{1}{\epsilon^2} (\xi^3 - \xi),$$

$$\text{ODE (no diffusion): } \dot{u} = -\frac{1}{\epsilon^2} f(u)$$

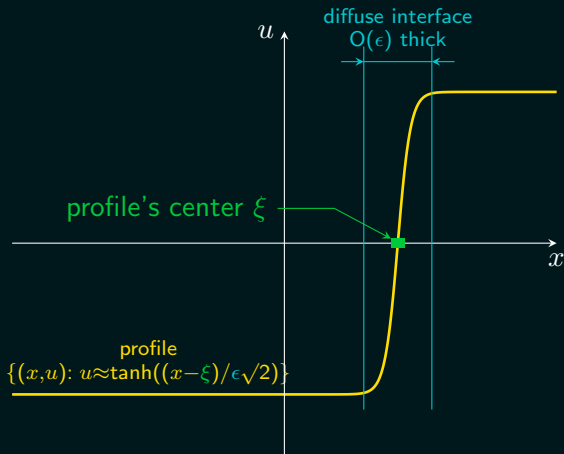
$$\text{equilibriums: } f(\pm 1) = 0, f(0) = 0,$$

$$\text{linearize: } \begin{array}{l} \pm 1 \text{ stable} - f'(\pm 1) < 0, \\ 0 \text{ unstable} - f'(0) > 0. \end{array}$$



Deterministic Allen–Cahn in 1 dimension

resolved profiles terminology



Deterministic Allen–Cahn in dimension $d > 1$

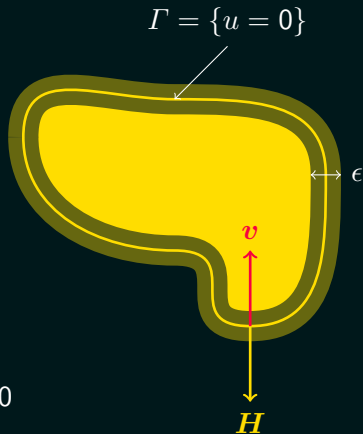
close relation to Mean Curvature Flow (MCF)

Level set $\Gamma = \{u = 0\}$, moves, as $\epsilon \rightarrow 0$
a **mean curvature flow**:

$$\epsilon \partial_t u|_{\Gamma} \quad -\epsilon \Delta u|_{\Gamma} \quad + \frac{1}{\epsilon} (u^3 - u)|_{\Gamma} = 0$$

$$\begin{array}{ccc} \downarrow & \downarrow & \downarrow \\ -v & -H & +0 = 0 \end{array}$$

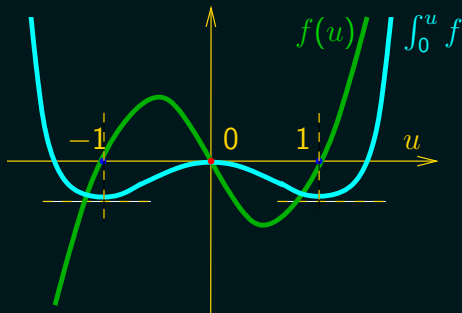
normal
velocity -mean
curvature



The Stochastic (or Noisy) Allen-Cahn Problem

is the following semilinear parabolic stochastic PDE with additive white noise

$$\begin{aligned}\partial_t u(x, t) - \Delta u(x, t) + f_\epsilon(u(x, t)) &= \epsilon^\gamma \partial_{xt} W(x, t), & x \in (0, 1), t \in \mathbb{R}^+. \\ u(x, 0) &= u_0(x), & x \in (0, 1) \\ \partial_x u(0, t) = \partial_x u(1, t) &= 0, & t \in \mathbb{R}^+.\end{aligned}$$



$f_\epsilon(\xi) = \frac{1}{\epsilon^2} (\xi^3 - \xi)$: first derivative of double well potential

$\epsilon \in \mathbb{R}^+$: “diffuse interface” parameter

$\gamma \in \mathbb{R}$: noise intensity parameter

$\partial_{xt} W$: space-time white noise

noise



White noise $\partial_{xt}W$: an informal definition

- Informally: **white noise** is mixed derivative of (2 dimensional) Brownian sheet $W = W_{x,t}$.
- **Brownian sheet W** : extension of 1-dim Brownian motion to multi-dim, built on Ω .
- Solutions of PDE understood as **mild solution**
- Notation for $\partial_{xt}W$

$$\int_0^\infty \int_0^1 f(x,t) dW(x,t) := \int_0^\infty \int_0^1 f(x,t) \partial_{xt}W(x,t) dx dt,$$

stochastic integral [Walsh, 1986].

- $\forall A \in \text{Borel}(\mathbb{R}^2) \int_A dW(x, t) =: W(A) \in \mathcal{N}(0, |A|)$, i.e, $W(A)$ is a 0-mean Gaussian random variable with variance = $|A|$.
- $A \cap B = \emptyset \Rightarrow W(A), W(B)$ independent and $W(A \cup B) = W(A) + W(B)$.
- Brownian sheet: $W_{x,t} = W([0, t] \times [0, x]) = \int_0^t \int_0^x dW(x, t)$.
- Basic yet crucial property:
$$\mathbb{E} \left[\left(\int_I \int_D f(x, t) dW(x, t) \right)^2 \right] = \mathbb{E} \left[\int_I \int_D f(x, t)^2 dx dt \right], \forall f \in L_2.$$

(Aka $dW = \sqrt{dx dt}$.)

Solutions of the stochastic linear heat equation

$$\begin{aligned}\partial_t w - \Delta w &= \partial_{xt} W, \text{ in } D \times \mathbb{R}_0^+ \\ w(0) &= 0, \text{ on } D \\ \partial_x w(1, t) &= \partial_x w(0, t) = 0, \forall t \in [0, \infty).\end{aligned}$$

Solution is defined as Gaussian process produced by the **stochastic integral**

$$Z_t(x) = Z(x, t) := \int_0^t \int_D G_{t-s}(x, y) dW(x, y).$$

where G is the heat kernel:

$$G_t(x, y) = 2 \sum_{k=0}^{\infty} \cos(\pi k x) \cos(\pi k y) \exp(-\pi^2 k^2 t).$$

(An “explicit semigroup” approach.)

Solutions of the stochastic Allen–Cahn problem

$$\begin{aligned}\partial_t u(x, t) - \Delta u(x, t) + f_\epsilon(u(x, t)) &= \epsilon^\gamma \partial_{xt} W(x, t), \text{ for } x \in D = [0, 1], t \in [0, \infty) \\ u(x, 0) &= u_0(x), \forall x \in D \\ \partial_x u(0, t) = \partial_x u(1, t) &= 0, \forall t \in \mathbb{R}^+.\end{aligned}$$

Defined as the continuous solution of integral equation

$$\begin{aligned}u(x, t) &= - \int_0^t \int_D G_{t-s}(x, y) f_\epsilon(u(y, s)) \, dy \, ds \\ &\quad + \int_D G_t(x, y) u_0(y) \, dy + \epsilon^\gamma Z_t(x).\end{aligned}$$

Unique continuous integral solution exists in 1d provided the initial condition u_0 fulfills boundary conditions.

Remarks on solution process

- The solution u of Stochastic Allen-Cahn, is adapted continuous Gaussian process (it is Hölder of exponents $1/2, 1/4$).
- The process u has continuous, but nowhere differentiable sample paths.
- This approach works only in $1d+time$, for higher dimensions; when defined solutions are extremely singular distributions (let alone continuous).
- If white noise (uncorrelated) is replaced by colored noise (correlated), then “regular” u can be sought in higher dimensions.
- Direct numerical discretization of this problem not obvious.

Discretization strategy

In two main steps:

1. **Replace white noise $\partial_{xt}W$ by a smoother object:** the approximate white noise $\partial_{xt}\bar{W}$.
2. **Discretize the approximate problem with $\partial_{xt}\bar{W}$** via a finite element scheme for the Allen-Cahn equation.

Inspired by [Allen et al., 1998], [Yan, 2005].

Approximate White Noise (AWN)

Fix a final time $T > 0$ and consider uniform **space and time partitions**

in space: $D = [0, 1]$, $D_m := (x_{m-1}, x_m)$, $x_m - x_{m-1} = \sigma$, $m \in [1 : M]$,

in time: $I = [0, T]$, $I_n := [t_{n-1}, t_n)$, $t_n - t_{n-1} = \rho$, $n \in [1 : N]$.

Regularization of the white noise is projection on piecewise constants:

$$\bar{\eta}_{m,n} := \frac{1}{\sigma\rho} \int_I \int_D \chi_m(x) \psi_n(t) \, dW(x, t).$$

$$\partial_{xt} \bar{W}(x, t) := \sum_{n=1}^N \sum_{m=1}^N \bar{\eta}_{m,n} \chi_m(x) \varphi_n(t).$$

$\chi_m = \mathbb{1}_{D_m}$, $\varphi_n = \mathbb{1}_{I_n}$ (characteristic functions).

$$\partial_{xt} \bar{W}(x, t) := \sum_{n=1}^N \sum_{m=1}^N \bar{\eta}_{m,n} \chi_m(x) \varphi_n(t).$$

$\bar{\eta}_{m,n}$ are independent $N(0, 1/(\sigma\rho))$ variables and

$$\mathbb{E} \left[\left(\int_I \int_D f(x, t) d\bar{W}(x, t) \right)^2 \right] \leq \mathbb{E} \left[\left(\int_I \int_D f(x, t) dW(x, t) \right)^2 \right].$$

$$\mathbb{E} \left[\left(\int_I \int_D d\bar{W}(x, t) \right)^2 \right] = T$$

$$\mathbb{E} \left[\int_I \int_D |\partial_{xt} \bar{W}(x, t)|^2 dx dt \right] \leq \frac{1}{\sigma\rho}$$

The regularized problem

$$\begin{aligned}\partial_t \bar{u} - \Delta \bar{u} + f_\epsilon(\bar{u}) &= \epsilon^\gamma \partial_{xt} \bar{W}, \\ \partial_x \bar{u}(t, 0) &= \partial_x \bar{u}(t, 1) = 0, \\ \bar{u}(0) &= u_0,\end{aligned}$$

Admits a “classical” solution. $\forall \omega \in \Omega \Rightarrow$ corresponding realization of the AWN $\partial_{xt} \bar{W}(\omega) \in L_\infty([0, T] \times D)$ (parabolic regularity) \Rightarrow $\partial_t \bar{u}(\omega) \in L_2([0, T]; L_2(D))$.

\Rightarrow variational formulation and thus **FEM** (or other standard methods) now possible.

Error estimate schedule:

1. Compare \bar{u} with u .
2. Approximate \bar{u} by U in a finite element space and compare.

The Finite Element Method

- Parameters (numerical mesh) $\tau, h > 0$ (approximation mesh) ρ, σ .
- Not necessary, but “natural” coupling: $\tau = \rho = h^2 = \sigma^2$.
- **Linearized Semi-Implicit Euler**

$$\begin{aligned} & \left\langle \frac{U^n - U^{n-1}}{\tau}, \Phi \right\rangle + \langle \partial_x U^n, \partial_x \Phi \rangle + \langle f'_\epsilon(U^{n-1})U^n, \Phi \rangle \\ &= \langle f'_\epsilon(U^{n-1})U^{n-1} + f_\epsilon(U^{n-1}), \Phi \rangle + \langle \epsilon^\gamma \partial_{xt} \bar{W}, \Phi \rangle, \quad \forall \Phi \in \mathbb{V}^h. \end{aligned}$$

\mathbb{V}^h is a finite element space of piecewise linear
[Kessler et al., 2004, Feng and Wu, 2005].

$$\left[\frac{1}{\rho} \mathbf{M} + \mathbf{A} + \frac{1}{\epsilon^2} \mathbf{N}(\mathbf{u}^{n-1}) \right] \mathbf{u}^n = \frac{1}{\epsilon^2} \mathbf{g}(\mathbf{u}^{n-1}) + \frac{1}{\rho} \mathbf{M} \mathbf{u}^{n-1} + \epsilon^\gamma \mathbf{w}.$$

- \mathbf{M} , \mathbf{A} usual mass and stiffness matrices,
- \mathbf{N} and \mathbf{g} nonlinear mass matrix and load vector
- $\mathbf{w} = (w_i)$ a **random load vector** generated at each time-step: for each node i we have

$$w_i = \frac{\epsilon^\gamma}{2} \sqrt{\frac{h}{\rho}} (\eta_{i-1} + \eta_i) \quad \eta_i \in \mathbf{N}(0, 1) \text{ pseudo-random.}$$

- Simple **Monte Carlo method** on \mathbf{w} .

Convergence of regularized to stochastic solution

Theorem (quasi-strong (least squares) convergence)

Let $\gamma > -1/2, T > 0$. For some c_1, c_2 ($\neq \epsilon$), and for each $\epsilon \in (0, 1)$ there correspond (i) an event Ω^∞ , (ii) constants C_ϵ, C_1, C_2 s.t.

$$P(\Omega^\infty) \geq 1 - 2c_1 \exp(-c_2/\epsilon^{1+2\gamma})$$

$$\int_{\Omega^\infty} \int_0^r \int_D |\bar{u} - u|^2 dx dt dP \leq C_\epsilon \left(C_1 \rho^{1/2} + C_2 \frac{\sigma^2}{\rho^{1/2}} \right), \forall \sigma, \rho > 0.$$

Remark

- 1 Event $\Omega^\infty = \{|u, \bar{u}| < 3\}$ (measured by maximum principle & exponential decay of “chi-squared” distribution).
- 2 C_ϵ grows exponentially with $1/\epsilon$.
- 3 Constant improves for $\gamma \gg 1$ (exploiting spectral gap).

Maximum principle in probability sense

Lemma

Suppose $\gamma > -1/2$. Given T , there exist $c_1, c_2, \delta_0 > 0$ such that if $\|u_0\|_{L^\infty(D)} \leq 1 + \delta_0$ then

$$P \left\{ \sup_{t \in [0, T]} \|(u, \bar{u})(t)\|_{L^\infty(D)} > 3 \right\} \leq c_1 \exp(-c_2/\epsilon^{1+2\gamma}).$$

Remark

- 1 The constant 3 is for convenience, can be replaced by $1 + \delta_1$, if needed, by adjusting c_1, c_2 and δ_0 .
- 2 This result is used to determine the event Ω^∞ for convergence to hold.
- 3 Because, nonlinearity is *not* globally Lipschitz.

Small noise resolution (for γ big: weak intensity)

Theorem (small noise)

Let q solution of *deterministic* the Allen–Cahn problem

$$\partial_t q - \Delta q + f_\epsilon(q) = 0, \quad q(0) = u_0, \quad \text{on } D.$$

Then $\forall T > 0 : \exists K_1(T) > 0, \epsilon_0(T) > 0$

$$P \left(\sup_{[0, T]} \|\bar{u} - q\|_{L_2(D)} \leq \epsilon^3 \right) \\ \geq 1 - \left(1 + \frac{K_1(T)}{2} \epsilon^{6-2\gamma} \right)^{T/(\sigma\rho)-1} \exp \left(-\frac{K_1(T)}{2} \epsilon^{6-2\gamma} \right)$$

for all $\epsilon \in (0, \epsilon_0)$, $\gamma > 3$ and $\rho, \sigma > 0$.

Theorem ([Chen, 1994], [de Mottoni and Schatzman, 1995])

Let q be the (classical) solution of the problem

$$\partial_t q - \Delta q + f_\epsilon(q) = 0, \quad q(0) = u_0, \quad \text{on } D$$

Key to argument in convergence for weak noise is the use of spectral estimate for q : There exists a constant $\lambda_0 > 0$ **independent of ϵ** such that for any $\epsilon \in (0, 1]$ we have

$$\|\partial_x \phi\|_{L_2(D)}^2 + \langle f'_\epsilon(q)\phi, \phi \rangle \geq -\lambda_0 \|\phi\|_{L_2(D)}^2, \quad \forall \phi \in H^1(D).$$

$X(0, T; L_2(D))$ bounds for AWN

Lemma

$\forall K > 0$

$$P \left\{ \sup_{t \in [0, T]} \|\partial_{xt} \bar{W}(t)\|_{L_2(D)} \leq K \right\} \\ \geq \left[1 - \frac{T}{\rho} \left(1 + \frac{K^2}{2} \rho \right)^{1/(2\sigma)-1} \exp \left(-\frac{K^2}{2} \rho \right) \right]^+$$

$$\text{and } P \left\{ \int_0^T \|\partial_{xt} \bar{W}(t)\|_{L_2(D)}^2 \leq K^2 \right\} \\ \geq 1 - \left(1 + \frac{K^2}{2} \right)^{1/(2\rho\sigma)-1} \exp \left(-\frac{K^2}{2} \right)$$

Convergence of FEM

Taking $\tau = \rho = h^2 = \sigma^2$ to simplify, we have

$$\int_{\Omega^\infty} \int_D |\bar{u}(t_n) - U^n|^2 dx dP \leq C(T, \epsilon)h.$$

Remark

- 1 compare w.r.t. deterministic case,
- 2 impossible to take E , but only \int_{Ω^∞} , due to rare events.

Theorem (Regularity of \bar{u})

$$\int_{\Omega^\infty} \int_{I_m} \int_D |\partial_t \bar{u}|^2 \, dx \, dt \leq c_1 \rho^{-1/2} + c_2 \sigma^{-1}$$
$$\int_{\Omega^\infty} \int_D |\Delta \bar{u}|^2 \, dx \leq c_3 \rho^{-3/2} + c_4 \sigma^{-1} \rho^{-1}.$$

For Ω^∞ an event of high probability.

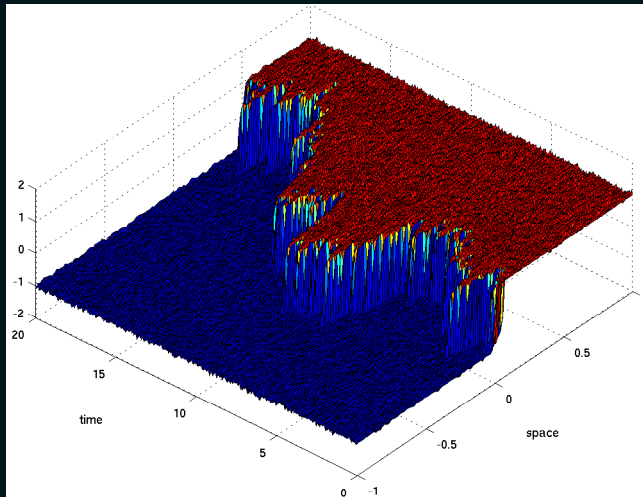
Remark

Expected loss of regularity, as $\sigma, \rho \rightarrow 0$.

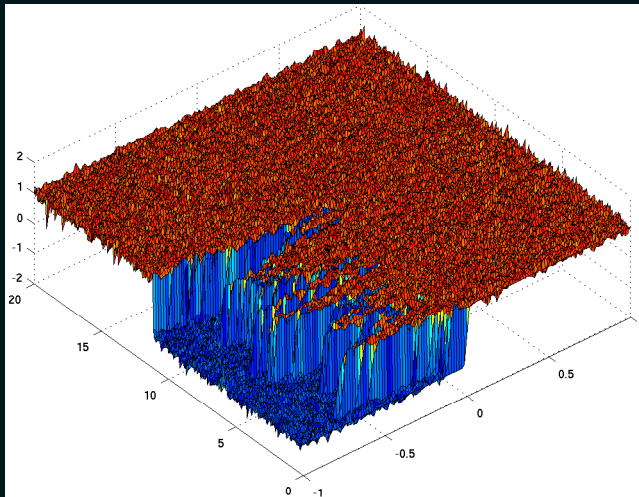
Numerical experiments

- 1 Computations for $\epsilon = 0.04, 0.02, 0.01$ and $\gamma = 1.0, 0.5, 0.2, 0.0, -0.2$ ($\gamma < 0$ though not discussed in theory can be interesting in practice).
- 2 Run a **Monte-Carlo** simulation for each set of parameters (2500 samples).
- 3 Meshsize $h < \epsilon$.
- 4 Timestep $\tau = c_0 h^2 \approx \epsilon^2$.

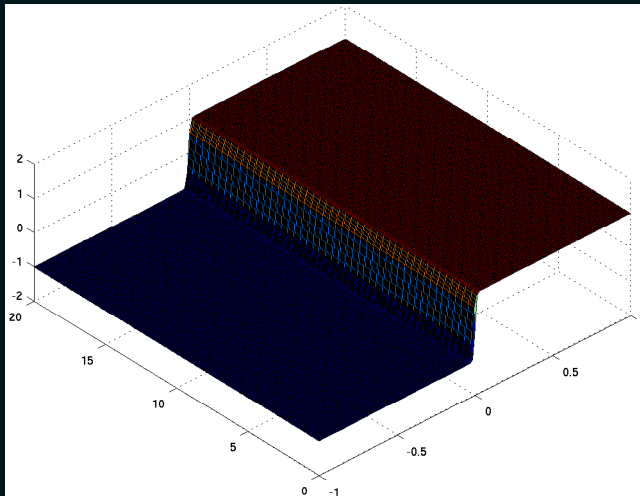
Sample path with $\epsilon = 0.01$, $\gamma = 0$



Sample path with $\epsilon = 0.01$, $\gamma = -0.2$



Sample path with $\epsilon = 0.01$, $\gamma = 1.0$



How to the benchmark our computations?

Benchmarking = “comparing with known solutions” Very few known “exact result”.

Theorem ([Funaki, 1995, Brassesco et al., 1995])

The interface motion is asymptotically, as $\epsilon \rightarrow 0$, a (1d) Brownian motion,

$$\lim_{\epsilon \rightarrow 0} P \left\{ \sup_{t \leq \epsilon^{-1-2\gamma}T} \left\| \tilde{u}_t - q(x - \tilde{\xi}_t^\epsilon) \right\|_{L_2(D)} > \delta \right\} = 0,$$

for $\delta > 0$.

Remark

- q is an **instanton** for the deterministic Allen-Cahn equation
- $\tilde{\xi}_t^\epsilon$ solves a **SODE** representing the motion of the interface
- $\tilde{u}_t(x)$ is an **appropriate rescaling** of $u(x, t)$.

- In our scaling, the interface position ξ_t performs a process that looks asymptotically (as $\epsilon \rightarrow 0$) like

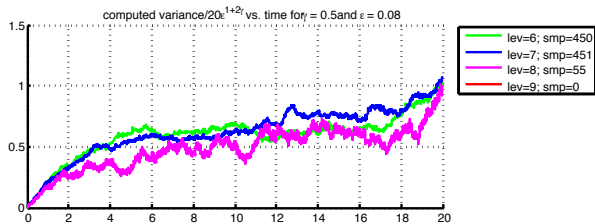
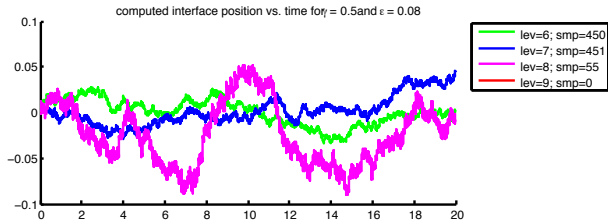
$$\xi_t^\epsilon \approx \frac{\sqrt{3}}{2\sqrt{2}} \epsilon^{\gamma+1/2} B_t,$$

where B_t is the 1d Brownian Motion.

We use **statistics on the interface** (discarding all cases of nucleation/coalescence).

Numerically computed **average** and **variance**

$$\gamma = 0.5 \text{ and } \epsilon = 0.08$$



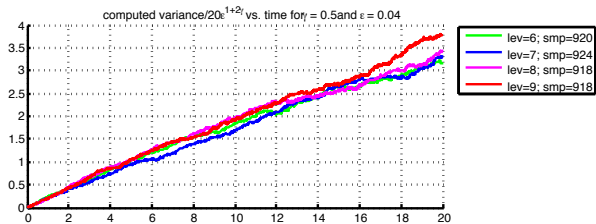
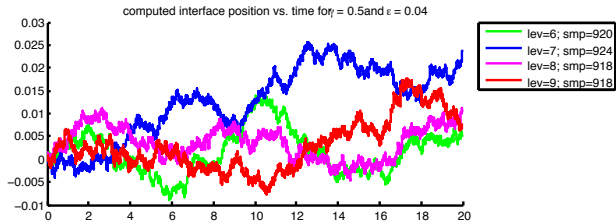
Average of Monte Carlo samples against time for various levels of refinement $\text{lev} = 6, 7, 8, 9$, and meshsize $h = 1/2^{\text{lev}}$.

Sample number smp differs with lev. Samples are **rejected** if annihilation/nucleation occurs.

Variance against time for the various levels. As time grows, variance accuracy deteriorates.

Numerically computed **average** and **variance**

$$\gamma = 0.5 \text{ and } \epsilon = 0.04$$



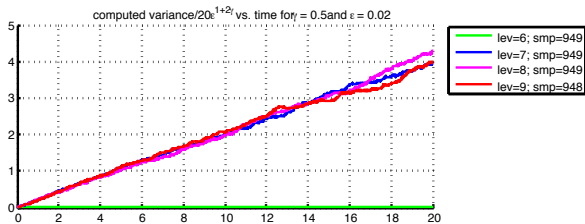
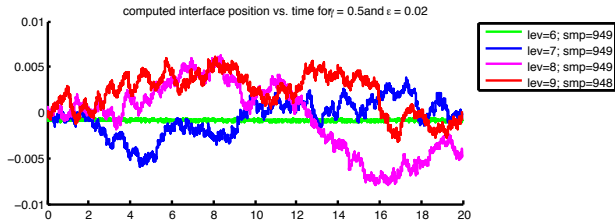
Average of Monte Carlo samples against time for various levels of refinement $\text{lev} = 6, 7, 8, 9$, and meshsize $h = 1/2^{\text{lev}}$.

Sample number smp differs with lev. Samples are **rejected** if annihilation/nucleation occurs.

Variance against time for the various levels. As time grows, variance accuracy deteriorates.

Numerically computed **average** and **variance**

$$\gamma = 0.5 \text{ and } \epsilon = 0.02$$



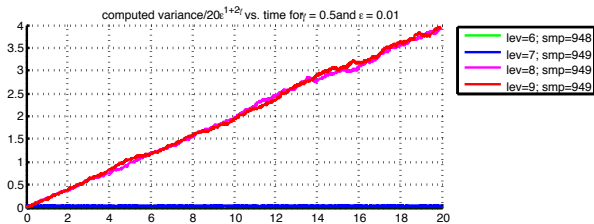
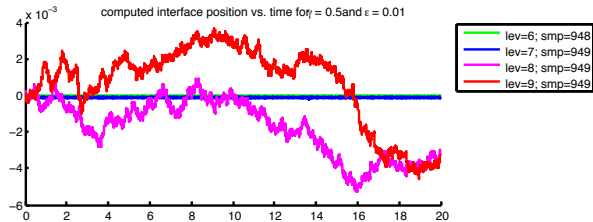
Average of Monte Carlo samples against time for various levels of refinement $\text{lev} = 6, 7, 8, 9$, and meshsize $h = 1/2^{\text{lev}}$.

Sample number smp differs with lev. Samples are **rejected** if annihilation/nucleation occurs.

Variance against time for the various levels. As time grows, variance accuracy deteriorates.

Numerically computed **average** and **variance**

$$\gamma = 0.5 \text{ and } \epsilon = 0.01$$



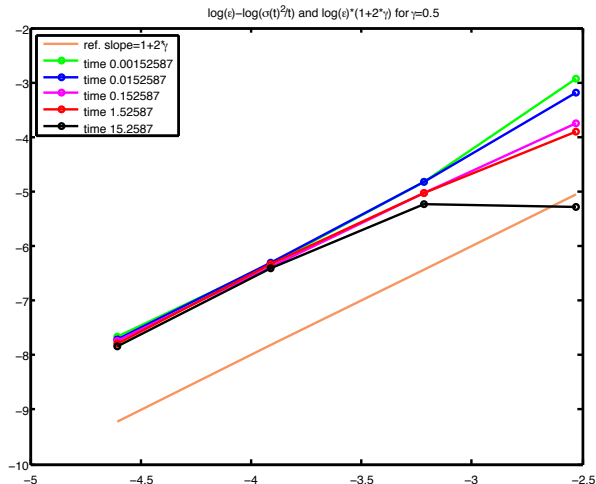
Average of Monte Carlo samples against time for various levels of refinement $\text{lev} = 6, 7, 8, 9$, and meshsize $h = 1/2^{\text{lev}}$.

Sample number smp differs with lev. Samples are **rejected** if annihilation/nucleation occurs.

Variance against time for the various levels. As time grows, variance accuracy deteriorates.

Simulations vs. theory

$\log(\text{var}[U_h^i] / t_i)$ vs. $\log \epsilon$ plot for $\gamma = 0.5$ at various times $t_i = t_0 10^i$



Theoretical slope (predicted by [Funaki, 1995] and [Brassesco et al., 1995]) is $1 + 2\gamma$.

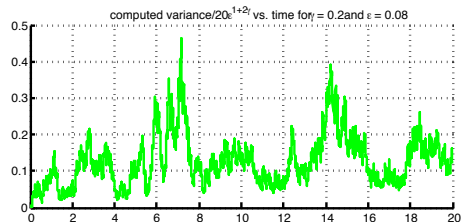
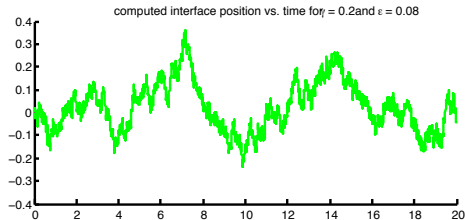
Plotted in **orange** reference line

As $\epsilon \rightarrow 0$ slope improves.

Meshsize $h = 1/512$.

Numerically computed **average** and **variance**

$$\gamma = 0.2 \text{ and } \epsilon = 0.08$$



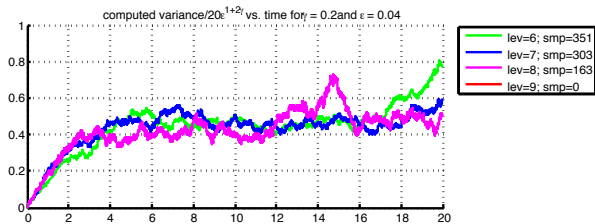
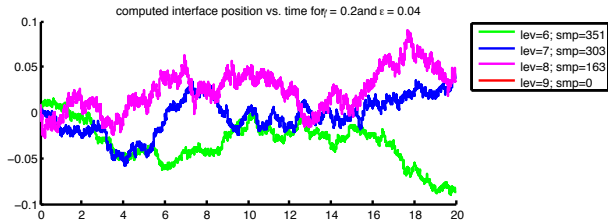
Average of Monte Carlo samples against time for various levels of refinement $\text{lev} = 6, 7, 8, 9$, and meshsize $h = 1/2^{\text{lev}}$.

Sample number smp differs with lev. Samples are **rejected** if annihilation/nucleation occurs.

Variance against time for the various levels. As time grows, variance accuracy deteriorates.

Numerically computed **average** and **variance**

$$\gamma = 0.2 \text{ and } \epsilon = 0.04$$



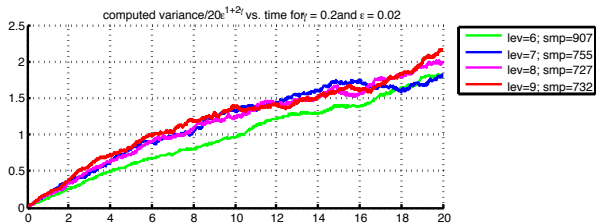
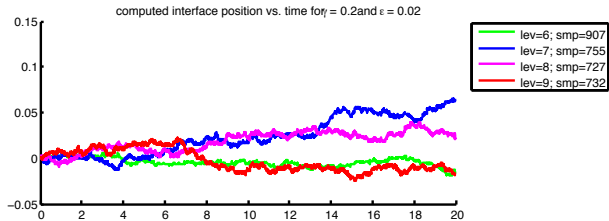
Average of Monte Carlo samples against time for various levels of refinement $\text{lev} = 6, 7, 8, 9$, and meshsize $h = 1/2^{\text{lev}}$.

Sample number smp differs with lev. Samples are **rejected** if annihilation/nucleation occurs.

Variance against time for the various levels. As time grows, variance accuracy deteriorates.

Numerically computed **average** and **variance**

$$\gamma = 0.2 \text{ and } \epsilon = 0.02$$



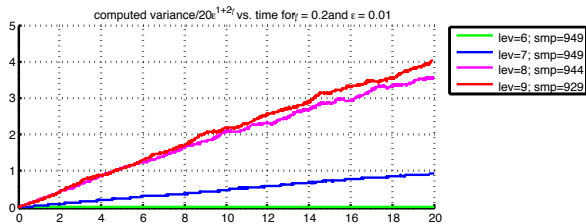
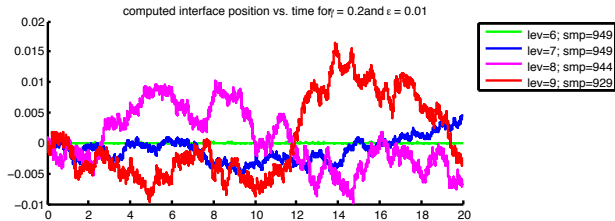
Average of Monte Carlo samples against time for various levels of refinement $\text{lev} = 6, 7, 8, 9$, and meshsize $h = 1/2^{\text{lev}}$.

Sample number smp differs with lev. Samples are **rejected** if annihilation/nucleation occurs.

Variance against time for the various levels. As time grows, variance accuracy deteriorates.

Numerically computed **average** and **variance**

$$\gamma = 0.2 \text{ and } \epsilon = 0.01$$



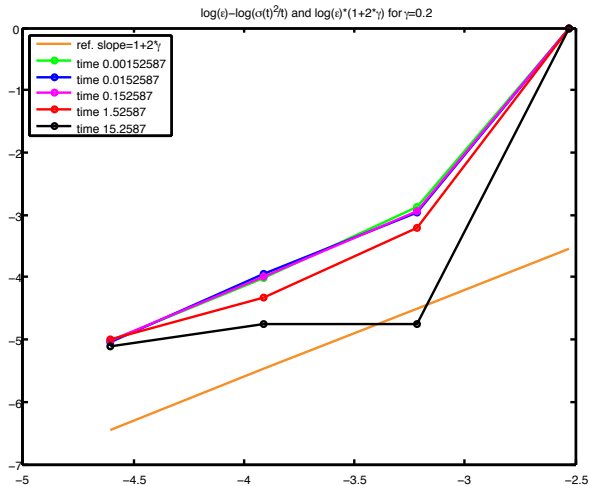
Average of Monte Carlo samples against time for various levels of refinement $\text{lev} = 6, 7, 8, 9$, and meshsize $h = 1/2^{\text{lev}}$.

Sample number smp differs with lev. Samples are **rejected** if annihilation/nucleation occurs.

Variance against time for the various levels. As time grows, variance accuracy deteriorates.

Simulations vs. theory

$\log(\text{var}[U_h^i] / t_i)$ vs. $\log \epsilon$ plot for $\gamma = 0.2$ at various times $t_i = t_0 10^i$



Theoretical slope (predicted by [Funaki, 1995] and [Brassesco et al., 1995]) is $1 + 2\gamma$.

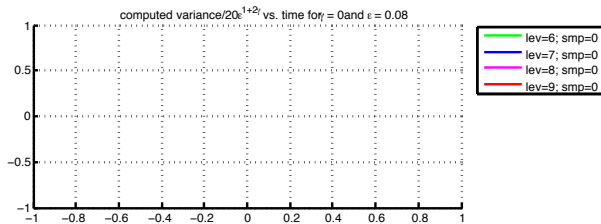
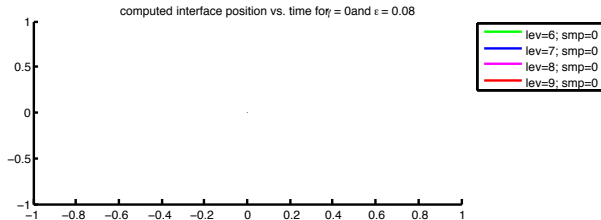
Plotted in **orange** reference line

As $\epsilon \rightarrow 0$ slope improves.

Meshsize $h = 1/512$.

Numerically computed **average** and **variance**

$$\gamma = 0.0 \text{ and } \epsilon = 0.08$$



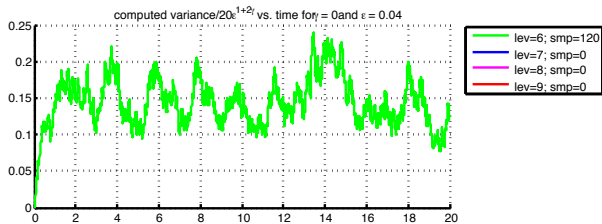
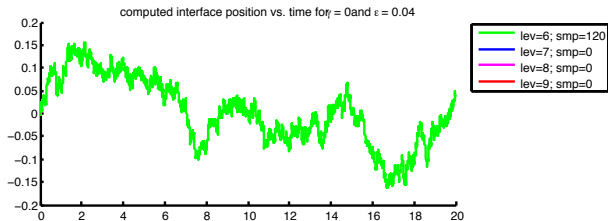
Average of Monte Carlo samples against time for various levels of refinement $\text{lev} = 6, 7, 8, 9$, and meshsize $h = 1/2^{\text{lev}}$.

Sample number smp differs with lev. Samples are **rejected** if annihilation/nucleation occurs.

Variance against time for the various levels. As time grows, variance accuracy deteriorates.

Numerically computed **average** and **variance**

$$\gamma = 0.0 \text{ and } \epsilon = 0.04$$



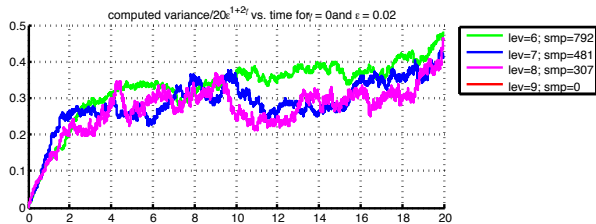
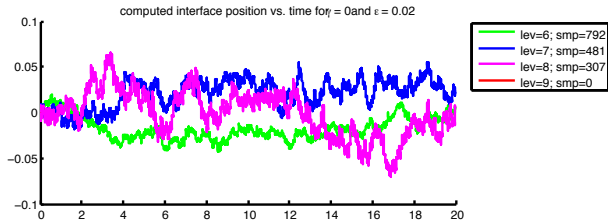
Average of Monte Carlo samples against time for various levels of refinement $\text{lev} = 6, 7, 8, 9$, and meshsize $h = 1/2^{\text{lev}}$.

Sample number smp differs with lev . Samples are **rejected** if annihilation/nucleation occurs.

Variance against time for the various levels. As time grows, variance accuracy deteriorates.

Numerically computed **average** and **variance**

$$\gamma = 0.0 \text{ and } \epsilon = 0.02$$



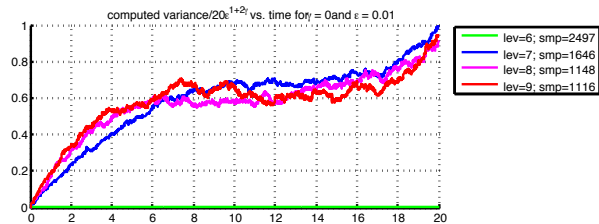
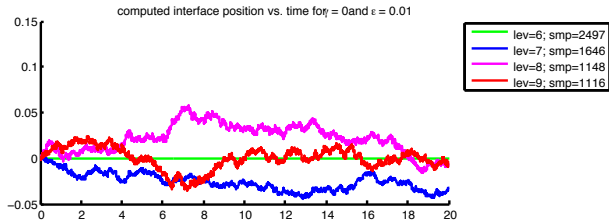
Average of Monte Carlo samples against time for various levels of refinement $\text{lev} = 6, 7, 8, 9$, and meshsize $h = 1/2^{\text{lev}}$.

Sample number smp differs with lev. Samples are **rejected** if annihilation/nucleation occurs.

Variance against time for the various levels. As time grows, variance accuracy deteriorates.

Numerically computed **average** and **variance**

$$\gamma = 0.0 \text{ and } \epsilon = 0.01$$



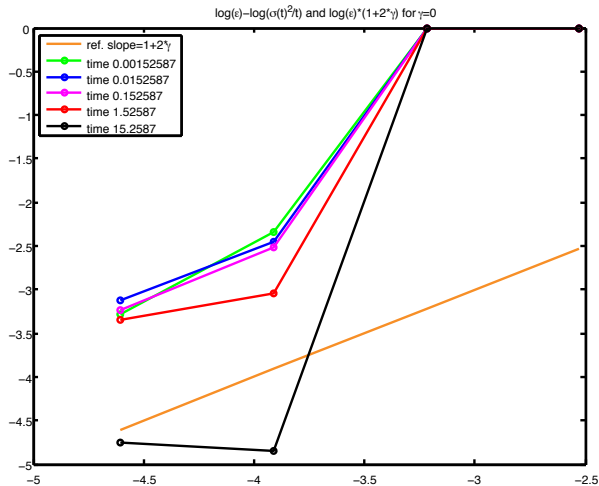
Average of Monte Carlo samples against time for various levels of refinement $\text{lev} = 6, 7, 8, 9$, and meshsize $h = 1/2^{\text{lev}}$.

Sample number smp differs with lev. Samples are **rejected** if annihilation/nucleation occurs.

Variance against time for the various levels. As time grows, variance accuracy deteriorates.

Simulations vs. theory

$\log(\text{var}[U_h^i] / t_i)$ vs. $\log \epsilon$ plot for $\gamma = 0.0$ at various times $t_i = t_0 10^i$



Theoretical slope (predicted by [Funaki, 1995] and [Brassesco et al., 1995]) is $1 + 2\gamma$.

Plotted in **orange** reference line

As $\epsilon \rightarrow 0$ slope improves.

Meshsize $h = 1/512$.

What we learned

- **Stability and convergence** numerical method for the stochastic Allen-Cahn in 1d.
- **Monte-Carlo** type simulations.
- **Benchmarking** via statistical comparison.
- **Adaptivity mandatory** (but different from “standard” phase-field approach) for higher dimensional study.

What we're trying to learn




Current investigation [Kossioris et al., 2009]

- finite ϵ “exact” solutions
- multiple interface convergence
- structure of the stochastic solution
- colored noise in $d > 1$
- adaptivity





What still needs to be learned

- Extension to Cahn-Hilliard type equations, Phase-Field, Dendrites.
- Other stochastic applications
- Chaos Expansion
- Kolmogorov (Fokker-Plank) equations
- Sparse methods





References I




-  Allen, E. J., Novosel, S. J., and Zhang, Z. (1998).
Finite element and difference approximation of some linear stochastic partial differential equations.
Stochastics Stochastics Rep., 64(1-2):117–142.
-  Allen, S. M. and Cahn, J. (1979).
A macroscopic theory for antiphase boundary motion and its application to antiphase domain coarsening.
Acta Metal. Mater., 27(6):1085–1095.
-  Brassesco, S., De Masi, A., and Presutti, E. (1995).
Brownian fluctuations of the interface in the $D = 1$ Ginzburg-Landau equation with noise.
Ann. Inst. H. Poincaré Probab. Statist., 31(1):81–118.




References II

-  Bronsard, L. and Kohn, R. V. (1990).
On the slowness of phase boundary motion in one space dimension.
Comm. Pure Appl. Math., 43(8):983–997.
-  Cahn, J. W. and Hilliard, J. E. (1958).
Free energy of a nonuniform system. I. Interfacial free energy.
Journal of Chemical Physics, 28(2):258–267.
-  Carr, J. and Pego, R. L. (1989).
Metastable patterns in solutions of $u_t = \epsilon^2 u_{xx} - f(u)$.
Comm. Pure Appl. Math., 42(5):523–576.
-  Chen, X. (1994).
Spectrum for the Allen-Cahn, Cahn-Hilliard, and phase-field equations
for generic interfaces.
Comm. Partial Differential Equations, 19(7-8):1371–1395.




References III

-  de Mottoni, P. and Schatzman, M. (1995). Geometrical evolution of developed interfaces. *Trans. Amer. Math. Soc.*, 347(5):1533–1589.
-  Dirr, N., Luckhaus, S., and Novaga, M. (2001). A stochastic selection principle in case of fattening for curvature flow. *Calc. Var. Partial Differential Equations*, 13(4):405–425.
-  Evans, L. C., Soner, H. M., and Souganidis, P. E. (1992). Phase transitions and generalized motion by mean curvature. *Comm. Pure Appl. Math.*, 45(9):1097–1123.
-  Faris, W. G. and Jona-Lasinio, G. (1982). Large fluctuations for a nonlinear heat equation with noise. *J. Phys. A*, 15:3025–3055.





-  Fatkullin, I. and Vanden-Eijnden, E. (2004).
Coarsening by diffusion-annihilation in a bistable system driven by noise.
Preprint, Courant Institute, New York University, New York, NY 10012.
-  Feng, X. and Wu, H.-j. (2005).
A posteriori error estimates and an adaptive finite element method for the Allen-Cahn equation and the mean curvature flow.
Journal of Scientific Computing, 24(2):121–146.
-  Funaki, T. (1995).
The scaling limit for a stochastic PDE and the separation of phases.
Probab. Theory Relat. Fields, 102:221–288.

-  Funaki, T. (1999).
Singular limit for stochastic reaction-diffusion equation and generation of random interfaces.
Acta Math. Sin. (Engl. Ser.), 15(3):407–438.
-  Fusco, G. and Hale, J. K. (1989).
Slow-motion manifolds, dormant instability, and singular perturbations.
J. Dynam. Differential Equations, 1(1):75–94.
-  Katsoulakis, M. A. and Szepessy, A. (2006).
Stochastic hydrodynamical limits of particle systems.
Commun. Math. Sci., 4(3):513–549.

References VI




-  Kessler, D., Nochetto, R. H., and Schmidt, A. (2004).
A posteriori error control for the Allen-Cahn problem: Circumventing Gronwall's inequality.
M2AN Math. Model. Numer. Anal., 38(1):129–142.
-  Kossioris, G., Lakkis, O., and Romito, M. (In preparation 2009).
Interface dynamics for the stochastic Allen–Cahn model: asymptotics and computations.
Technical report.
-  Liu, D. (2003).
Convergence of the spectral method for stochastic Ginzburg-Landau equation driven by space-time white noise.
Commun. Math. Sci., 1(2):361–375.

References VII

-  Lythe, G. (1998).
Stochastic PDEs: domain formation in dynamic transitions.
In *Proceedings of the VIII Reunión de Física Estadística, FISES '97*,
volume 4, pages 55—63. Anales de Física, Monografías RSEF.
-  Nestler, B., Danilov, D., and Galenko, P. (2005).
Crystal growth of pure substances: phase-field simulations in
comparison with analytical and experimental results.
J. Comput. Phys., 207(1):221–239.
-  Rubinstein, J., Sternberg, P., and Keller, J. B. (1989).
Fast reaction, slow diffusion, and curve shortening.
SIAM J. Appl. Math., 49(1):116–133.
-  Shardlow, T. (2000).
Stochastic perturbations of the Allen-Cahn equation.
Electron. J. Differential Equations, pages No. 47, 19 pp. (electronic).



References VIII

-  Souganidis, P. E. and Yip, N. K. (2004).
Uniqueness of motion by mean curvature perturbed by stochastic noise.
Ann. Inst. H. Poincaré Anal. Non Linéaire, 21(1):1–23.
-  Walsh, J. B. (1986).
An introduction to stochastic partial differential equations.
In *École d'été de probabilités de Saint-Flour, XIV—1984*, volume 1180 of *Lecture Notes in Math.*, pages 265–439. Springer, Berlin.
-  Warren, J. and Boettinger, W. (1995).
Prediction of dendritic growth and microsegregation in a binary alloy using the phase-field method.
Acta Metall. Mater., 43(2):689–703.



Yan, Y. (2005).

Galerkin finite element methods for stochastic parabolic partial differential equations.

SIAM J. Numer. Anal., 43(4):1363–1384 (electronic).